Pure Appl. Chem., Vol. 81, No. 10, pp. 1903–1920, 2009.
doi:10.1351/PAC-CON-08-10-04

Thermodynamics in an icy world: The atmosphere and internal structure of Saturn's moon Titan*,**

Andreas Heintz‡ and Eckard Bich

Department of Physical Chemistry, University of Rostock, Rostock, Germany

Abstract: Thermodynamic principles can be applied for describing the atmospheres and the internal structure of celestial bodies using Saturn's moon Titan as a most appropriate example.

Some basic physical data of Titan such as the measured temperature and pressure on its surface, the atmospheric composition, Titan's density and diameter, and other information allow us to predict further properties which have not been determined directly by measurements. The existence of a liquid phase covering smaller parts of the surface can be confirmed, and the composition of the liquid can be predicted. The change of temperature with the height over the surface and the appearance of clouds and rainfall in the atmosphere consisting essentially of $CH_4 + N_2$ mixtures can also be predicted. By developing a new method of calculation of atmospheric scenarios, the chemical history of Titan's surface and atmosphere can be roughly reconstructed taking into account the known rate of methane destruction caused by radiative absorption of sunlight. Finally, some estimations concerning the material structure and the pressure behavior of Titan's interior can be made. Only basic knowledge of thermodynamics and physics is required to understand essential features in a strange world that is more than one billion kilometers away from us.

Keywords: thermodynamics; Saturn; Titan; Cassini–Huygens; Titan atmosphere.

INTRODUCTION

The atmosphere and internal structure of the icy satellites of Jupiter and Saturn offer the most interesting subject for studying their thermodynamic properties. This can be done even at a level that is accessible for graduate students. The treatment provides a motivating example of applying thermodynamic and physical principles beyond the well-known classical areas of chemical engineering and chemical separation or reaction processes.

Particularly, Saturn's largest moon Titan is most suitable for that purpose for several reasons. Numerous data of Titan have been obtained by observations from Earth, from the Voyager 1 and 2 missions in 1977 and most recently from the Cassini–Huygens mission which in particular provided the most spectacular results in the years 2005–2008:

- Titan has a dense atmosphere consisting mainly of N_2 (93–98 %) and methane (7–2 %) with a pressure of 1.5 bar and a temperature of –180 °C = 93 K at the bottom.

*Paper based on a presentation at the 20th International Conference on Chemical Thermodynamics (ICCT 20), 3–8 August 2008, Warsaw, Poland. Other presentations are published in this issue, pp. 1719–1959.

**Dedicated to Prof. Dr. Eckhard Vogel on the occasion of his 65th birthday.

‡Corresponding author: Tel: +49-381-498-6500; Fax: +49-381-498-6502; E-mail: andreas.heintz@uni-rostock.de

- Methane plays a similar role on Titan as water on Earth, causing similar meteorological processes.
- Liquid lakes consisting of the atmospheric components cover at least 4 % of Titan's surface, maybe even more, because only parts of Titan's surface have been investigated so far by the Cassini probe.
- Solid water ice plays a similar role as rocky material and sediments on Earth's surface.
- Due to its low density (1.88 g m^{-3}), Titan must contain remarkable amounts of water in its mantle while its inner core consists of rocky material.

Important questions arise which can be answered by thermodynamic methods as shown in the following sections:

- What is the composition of the condensed liquid phase on Titan's surface?
- What does the temperature profile of the atmosphere look like and what role does methane play in the formation of clouds and rainfall?
- How have the atmosphere and surface developed in the past and what will be their future fate?
- What can be said about Titan's internal structure?

Table 1 gives some information on physical properties and interplanetary data of Titan.

Table 1 Physical parameters of Titan.

Mass/kg	Radius/km	Gravity acceleration/m s^{-2}	Average density/g m^{-3}	Rotational period/days
$1.344 \cdot 10^{23}$	2575	1.354	1.88	16
Surface temperature/K	Surface pressure/bar	Surface area/m^2	Distance to sun/km	Distance to Saturn/km
93	1.49	$8.332 \cdot 10^{13}$	$1.428 \cdot 10^{9}$	$1.222 \cdot 10^{9}$

Titan always turns the same side to Saturn, i.e., its rotational period is identical with its revolution time around Saturn. Much more detailed information than presented in this article can be found in the literature [1–15].

PHOTOCHEMISTRY IN TITAN'S ATMOSPHERE

The most important gaseous components detected and determined quantitatively in Titan's atmosphere are presented in Table 2.

Table 2 Atmospheric composition in mol % [2].

N_2	CH_4	H_2	CO	C_2H_6	C_2H_2	C_2H_4	HCN
93–98	7–2	0.1	$6 \cdot 10^{-3}$	$2 \cdot 10^{-3}$	$2 \cdot 10^{-4}$	$4 \cdot 10^{-5}$	$2 \cdot 10^{-5}$

The atmosphere is characterized by clouds in the troposphere and a hazy upper atmosphere containing aerosol particles of ~1 μm size which conceals a free view of Titan's surface in the visible region of light. However, UV, IR, and mainly radar imaging technique is able to reveal details of Titan's atmosphere and surface. This situation indicates an intensive photochemical activity in the atmosphere. A simplified version of the photochemical destruction processes caused by solar UV-irradiation reads as follows [2–5]:

$$2CH_4 + h\nu \rightarrow C_2H_6 + H_2 \quad \text{(reaction I)}$$

$$2CH_4 + h\nu' \rightarrow C_2H_4 + 2H_2 \quad \text{(reaction II)}$$

$$C_2H_4 + h\nu'' \rightarrow C_2H_2 + H_2 \quad \text{(reaction IIb)}$$

$$2CH_4 \rightarrow C_2H_2 + 3H_2 \quad \text{(reaction II = IIa + IIb)}$$

$$2CH_4 + h\nu''' \rightarrow \tfrac{2}{n}C_nH_2 + (4 - \tfrac{2}{n})\,H_2 \quad \text{(reaction III)}$$

This reaction scheme shows that the appearance of C_2H_6 and C_2H_2 in the atmosphere (Table 2) has its origin in the photochemistry of C_2H_6. C_2H_2 is a photochemically unstable intermediate product. The haze in the upper atmosphere is mainly caused by the production of polyenes (reaction III). H_2 escapes rapidly from the atmosphere into the space due to Titan's low escape velocity. It is assumed that ca. 80 % of the destructed CH_4 is transformed into C_2H_6, ca. 12 % into C_2H_2, and 8 % into polyenes [2,11]. C_2H_6 is assumed to be dissolved partly in the liquid lakes on the surface. Most of C_2H_6 and all other photochemical products remain as small particles in the atmosphere (polyenes) or are adsorbed on the icy surface on the bottom.

COMPOSITION OF LAKES ON TITAN'S SURFACE

The discovery of liquid lakes with areas up to the size of Lake Superior (USA) was one of the most spectacular results of the Cassini mission [6–8]. What is the composition of these lakes covering at least several percent of the surface? The simplest assumption is that these lakes consist of a liquid mixture of N_2 and CH_4, which are also the dominant components in the gaseous atmosphere. It is an easy task to calculate the liquid composition treating the binary system as an ideal liquid mixture. We only have to know the temperature of the lakes and the saturation pressure. Obvious choices are the experimentally determined surface temperature of $T = 93$ K and the total surface pressure $p = 1.49$ bar. According to Raoult's ideal law, it follows

$$p \cdot y_{CH_4} = p^{sat}_{CH_4} \cdot x_{CH_4} \text{ and } p \cdot y_{N_2} = p^{sat}_{N_2}\left(1 - x_{CH_4}\right) \tag{1}$$

with the mole fractions y_i and x_i in the gaseous atmosphere and in the liquid phase, respectively (i = CH_4, N_2).

The saturation pressures of methane and nitrogen at 93 K are [16,17,24]

$$p^{sat}_{CH_4} = 0.1598 \text{ bar}, \; p^{sat}_{N_2} = 4.625 \text{ bar}$$

Using these data, we obtain

$$x_{CH_4} = \frac{p - p^{sat}_{N_2}}{p^{sat}_{CH_4} - p^{sat}_{N_2}} = 0.698 \text{ and } x_{N_2} = 1 - x_{CH_4} = 0.302 \tag{2}$$

The predicted composition of the atmosphere is therefore

$$\begin{aligned} y_{CH_4} &= p^{sat}_{CH_4} \cdot x_{CH_4} \,/\, p = 0.074 \\ y_{N_2} &= p^{sat}_{N_2} \cdot x_{N_2} \,/\, p = 0.926 \end{aligned} \tag{3}$$

This is close to the experimental data of y_{N_2} (0.93–0.98) and y_{CH_4} (0.02–0.07) and suggests that the predicted composition of the lakes with 70 mol % CH_4 and 30 mol % N_2 is no unreasonable result.

However, there are serious arguments in the literature that the liquid phase of the lakes and also humidity in the pores of the solid water ice on the bottom may contain also considerable amounts of ethane (C_2H_6) [8–12] since C_2H_6 is soluble in liquid CH_4 or liquid $CH_4 + N_2$ mixtures. Therefore, a more refined model of the ternary system $CH_4 + N_2 + C_2H_6$ has to be applied accounting also for non-ideality of the three mixture components in the liquid as well as in the gaseous phase.

We start with the following expression for the total pressure p of a real liquid ternary mixture being in thermodynamic equilibrium with its real gaseous phase (C = CH_4, N = N_2, E = ethane = C_2H_6).

$$p = \left(x_C \gamma_C\right) \cdot \left(\pi_C \cdot p_C^{sat}\right) + \left(x_N \gamma_N\right) \cdot \left(\pi_N \cdot p_N^{sat}\right) + \left(x_E \gamma_E\right) + \left(\pi_E \cdot p_E^{sat}\right) \tag{4}$$

$\gamma_i (i = C,N,E)$ and $\pi_i (i = C,N,E)$ are the activity coefficients of i in the liquid phase and the so-called Poynting correction factors for component i, respectively. Equation 4 exhibits a sufficiently correct description of ternary vapor–liquid phase equilibria provided the reality of the gaseous phase can be described by accounting for second virial coefficients B_i and the approximation is acceptable that all activity coefficients in the vapor phase are unity (Lewis–Randall rule in the vapor phase).

γ_i and π_i are given by the following equations:

$$\begin{aligned} RT \ln\gamma_C &= a_{CN} \cdot x_N(1 - x_C) + a_{CE}(1 - x_C)x_E - a_{NE}x_N \cdot x_E \\ RT \ln\gamma_N &= a_{CN} \cdot x_C(1 - x_N) + a_{NE}(1 - x_N)x_E - a_{CE}x_C \cdot x_E \\ RT \ln\gamma_E &= a_{CE} \cdot x_C(1 - x_E) + a_{NE}(1 - x_E)x_N - a_{CN}x_C \cdot x_N \end{aligned} \tag{5}$$

with the balance for mole fractions

$$x_C + x_N + x_E = 1$$

and the Poynting factors

$$\pi_i = \exp\left[\frac{\left(\bar{V}_{i,l} - B_i\right)\left(p - p_i^{sat}\right)}{RT}\right] \quad \left(i = C,N,E\right) \tag{6}$$

The parameters a_{ij} characterize the difference of intermolecular interactions in binary liquid mixtures $i + j$ and are based on the simple expression for the molar Gibbs excess enthalpy G_{ij}^E of the binary mixture $i + j$:

$$G_{ij}^E = a_{ij} x_i x_j$$

The Gibbs excess enthalpy of the ternary mixture is

$$G_{ter}^E = RT\left(x_C \ln\gamma_C + x_N \ln\gamma_N + x_E \ln\gamma_E\right) \tag{7}$$

with ln γ_i from eq. 5.

Parameters a_{CN}, a_{CE}, and a_E can be obtained from experimental data of binary G_{ij}^E available from the literature [19–21] by fitting eq. 7 to the experiments. Values obtained are listed in Table 3. Calculation of π_i in eq. 6 requires data of the liquid molar volume $\bar{V}_i^l$ [22,23] and the second virial coefficient B_i [17,18,24] for each component at $T = 93$ K. Values are also listed in Table 3.

Table 3 Thermodynamic parameters of the ternary mixture components at 93 K.

a_{CN}/J mol^{-1}	a_{CE}/J mol^{-1}	a_{NE}/J mol^{-1}
720	440	800
$V^l_{CH_4}$/m^3·mol^{-1}	$V^l_{N_2}$/m^3·mol^{-1}	$V^l_{C_2N_6}$/m^3·mol^{-1}
35.65	38.42	67.83
B_{CH_4}/m^3·mol^{-1}	B_{N_2}/m^3·mol^{-1}	$B_{C_2N_6}$/m^3·mol^{-1}
–455	–186	–2500

At given liquid composition x_C, x_N, and $x_E = 1 - x_E - x_N$, γ_C, γ_N, and γ_E can be calculated using eq. 5. π_C, π_N, and π_E can be calculated by eq. 6 using $p = 1.49 \cdot 10^5$ Pa and the known values of p_i^{sat}. Compositions $y_i (i = C,N,E)$ are than obtained by

$$y_i = x_i \gamma_i p_i^{sat} \cdot \pi_i \quad (i = C,N,E) \tag{8}$$

It turns out that $y_E \approx 0$ for almost all compositions x_C and x_N due to the negligible vapor pressure $p_E^{sat} = 2.3 \cdot 10^{-5}$ bar [18] compared to p_C^{sat} and p_N^{sat} at 93 K. As a result, the vapor phase can be treated as a binary mixture of CH_4 and N_2. For presenting our results of the ternary liquid mixture in Fig. 1 the mole fractions in the liquid state x_C, x_N, and $x_E = 1 - x_C - x_N$ are plotted as a function of the composition of $y_{CH_4} \cong 1 - y_{N_2}$ up to $y_{CH_4} = 0.1$. Figure 1 shows that x_E is continuously decreasing with increasing y_C while x_C is continuously increasing. At $y_{CH_4} \cong 0.10$, $x_E = 0$, i.e., values of $y_{CH_4} \geq 0.1$ would indicate that no ethane can be present in the liquid phase. Interestingly, x_N is almost independent of y_C with values close to 0.18. The following conclusions can be drawn from Fig. 1. Since experimental values of y_{CH_4} lie between 0.02 and 0.07, the results suggest that ethane would be present in the liquid phase with values of x_E in the range of 0.7–0.2. However, there is no evidence that the measured values of y_{CH_4} are really values being in thermodynamic equilibrium with a saturated liquid mixture at the places where these values have been measured in Titan's atmosphere. Therefore, equilibrium values of y_{CH_4} which are representative for the liquid composition of the lakes may reach or even exceed 0.1. In this case, most likely no ethane would be present in the lakes and the liquid composition would be

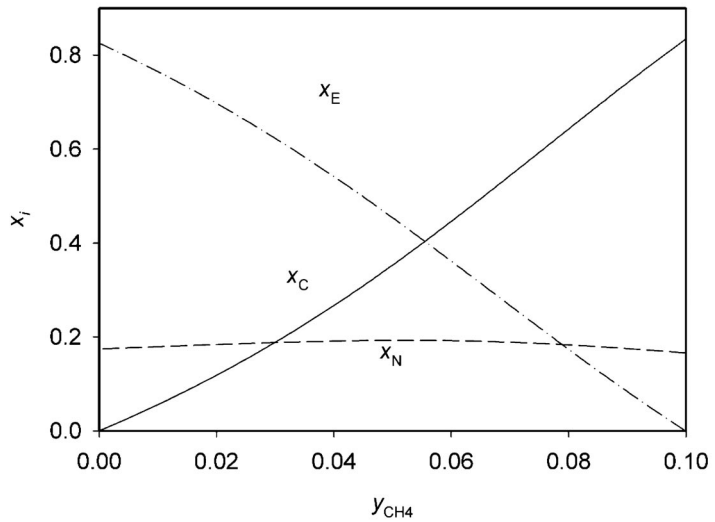

Fig. 1 Liquid composition $x_i (i = C,N,E)$ of the ternary system $CH_4 + N_2 + C_2H_6$ as function of mole fraction of methane, y_C, in a saturated atmosphere.

$x_{CH_4} \cong 0.834$ and $x_{N_2} \cong 0.166$, which is different from the result obtained by eq. 2 under the assumption of an ideal binary mixture ($x_{CH_4} = 0.698$, $x_{N_2} = 0.302$).

CLOUD FORMATION AND RAINFALL IN TITAN'S TROPOSPHERE

Early attempts to describe quantitatively the situation of a saturated atmosphere of Titan can be found in the literature [25,26]. We provide here a simple and straightforward procedure based on the most recent results of the temperature profile of the lower atmosphere.

Figure 2 shows the temperature profile of Titan's atmosphere as measured by the landing probe Huygens [14]. The relatively high temperatures in the thermosphere are caused by the absorption of solar radiation. This is the region where the photochemical processes take place. At ca. 40 km the temperature reaches a minimum value of ca. 73 K, increasing again below this altitude. The nearly linear temperature profile below 20 km is called the polytropic lapse rate. Its slope (dT/dh) is negative (–0.92 K km^{-1}). This is the part of the troposphere where cloud formation of $CH_4 + N_2$ mixtures can take place as well as rainfall. Such negative lapse rates of temperature are also observed in other dense atmospheres, e.g., on Earth or on Venus, and can be explained by the convection of gases in a gravitational field which corresponds approximately to an isentropic process which is given by the following differential relationship valid for ideal gases:

$$\frac{dT}{T} = \frac{\gamma - 1}{\gamma}\frac{dp}{p} \quad \text{with } \gamma = C_p / C_V \tag{9}$$

C_p and C_V are the molar heat capacities at constant pressure and volume, respectively.

Real processes are often better described by ε instead of γ with

$$1 \le \varepsilon \le \gamma \tag{10}$$

ε is called the polytropic coefficient.

Considering hydrostatic equilibrium as a necessary condition in any atmosphere, we have for ideal gases

$$dp = -p\frac{\bar{M} \cdot g}{RT}dh \tag{11}$$

where $\bar{M}$ is the average molar mass of the gas and h is the altitude.

Combining eq. 9 with eq. 11 and using ε instead of γ integration gives the temperature profile in the atmosphere

$$T(h) = T_0\left(1 - \frac{\bar{M} \cdot g}{R}\frac{\varepsilon - 1}{\varepsilon}\frac{h}{T_0}\right) \tag{12}$$

with $\bar{M} = 0.028$ kg mol^{-1}, $T_0 = 93$ K, and g = 1.354 m s^{-1} (see Table 1).

Substituting eq. 12 into eq. 9 integration gives the pressure profile in the atmosphere

$$p(h) = p_0\left(1 - \frac{\bar{M} \cdot g}{R}\frac{\varepsilon - 1}{\varepsilon}\frac{h}{T_0}\right)^{\frac{\varepsilon}{\varepsilon - 1}} = p_0\left(\frac{T(h)}{T_0}\right)^{\frac{\varepsilon}{\varepsilon - 1}} \tag{13}$$

with $p_0 = 1.49 \cdot 10^5$ Pa.

The experimental lapse rate (dT/dp) = –0.92 K km^{-1} is best described by eq. 12 with $\varepsilon = 1.25$. It is worth noting that eq. 13 gives the barometric formula for an isothermic atmosphere with $T = T_0$ in the limiting case of $\lim_{\varepsilon \to 1}$ (eq. 13).

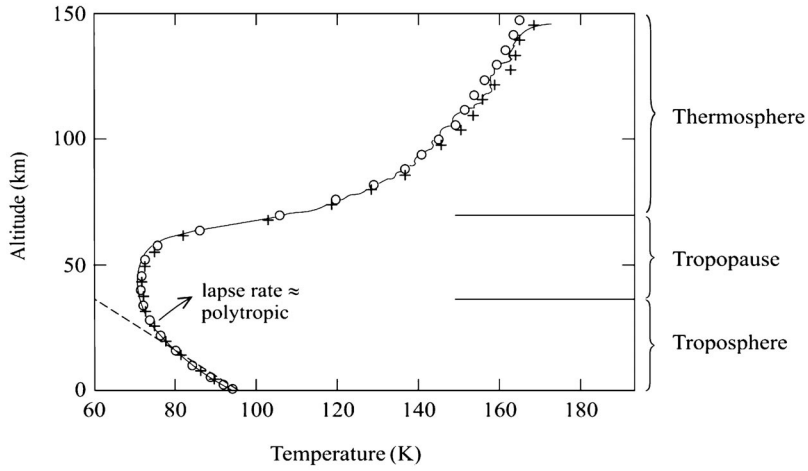

Fig. 2 Temperature profile in Titan's atmosphere (see text).

We are now prepared to develop a straightforward procedure for calculating cloud formation based on the assumption of a real binary mixture in the liquid state consisting of CH_4 and N_2. By equating eq. 4 with $x_{\text{Ethane}} = 0$ and eq. 13 we obtain

$$p(h) = x_{CH_4} \cdot \gamma_{CH_4} \cdot \pi_{CH_4} \cdot p^{\text{sat}}_{CH_4}\left[T(h)\right] + \left(1 - x_{CH_4}\right) \cdot \gamma_{N_2} \pi_{N_2} \cdot p^{\text{sat}}_{N_2}\left[T(h)\right] = p_0 \left[1 - \frac{\bar{M} \cdot g}{R} \cdot \frac{\varepsilon - 1}{\varepsilon} \frac{h}{T_0}\right]^{\frac{\varepsilon}{\varepsilon - 1}} \tag{14}$$

Substituting now $T(h)$ from eq. 12 into the left-hand side of eq. 14 gives x_{CH_4} of the saturated $CH_4 + N_2$ mixture as function of the altitude h. The corresponding mole fraction y_{CH_4} is calculated by

$$y_{CH_4} = \frac{x_{CH_4} \cdot \gamma_{CH_4} \cdot p^{\text{sat}}_{CH_4}\left[T(h)\right] \cdot \pi_{CH_4}}{p(h)} \tag{15}$$

where $p(h)$ is eq. 14.

Results are shown in Fig. 3, which also shows the temperature profile (eq. 12) and the solid–liquid equilibrium of methane. Figure 3 demonstrates that only values of y_{CH_4} **below** the $y_{CH_4}(h)$ curve represent a dry atmosphere. For $y_{CH_4} > y_{CH_4}(h)$ phase splitting, i.e., condensation occurs, e.g., for y = 0.049 above 8700 m or for y = 0.036 above 12 000 km. These are the cloud heights where we also can expect rainfall provided there is no supersaturation. Figure 3 also shows that "methane snow" will never occur in Titan's atmosphere since the solid–liquid line of CH_4 does not intersect the $x_{CH_4}(h)$ curve above the temperature minimum of 73 K (Fig. 2) due to the freezing point depression of the $CH_4 + N_2$ mixture, $y_{CH_4} = 0.0975$ and $x_{CH_4} = 0.834$ are the saturation values at the bottom as already calculated for the real model in the third section.

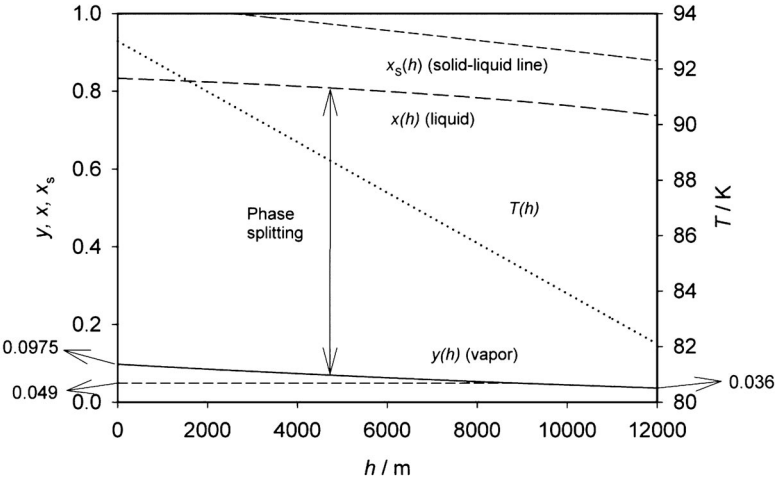

Fig. 3 Composition profile in a polytropic atmosphere (see text).

APPROXIMATIVE SCENARIO OF TITAN'S ATMOSPHERE IN THE PAST AND IN THE FUTURE

To our knowledge, no attempts have been made so far to develop a thermodynamically consistent procedure of a time-dependent scenario of Titan's atmosphere.

The simplified scenario presented here is based on the assumption that the gaseous atmosphere as well as the liquid reservoirs on Titan's surface consist of binary CH_4 + N_2 mixtures which behave as ideal gases in the vapor phase and obey Raoult's ideal law. Further, we assume that the total amount of N_2 remains unchanged over the time, only CH_4 underlies a photochemical destruction process occurring exclusively in the gaseous phase, i.e., in the atmosphere, with a known destruction rate constant. The photokinetic process is assumed to be slow compared to the rate for establishing the thermodynamic phase equilibrium. Starting with the mole numbers of CH_4, $n^g_{CH_4}$, and N_2, $n^g_{N_2}$ in the atmospheric (gaseous) phase given by the force balances between gravitational forces and pressure forces at $h = 0$

$$n^g_{CH_4} = \frac{p^{sat}_{CH_4} \cdot A}{M_{CH_4} \cdot g} x_{CH_4} \quad \text{and} \quad n^g_{N_2} = \frac{p^{sat}_{N_2} \cdot A}{M_{N_2} \cdot g}\left(1 - x_{CH_4}\right) \tag{16}$$

the total mole fraction of methane $\bar{x}_{CH_4}$ being an averaged value of **both** phases is

$$\bar{x}_{CH_4} = \frac{n^l_{CH_4} + x_{CH_4} \cdot \dfrac{p^{sat}_{CH_4} \cdot A}{M_{CH_4} \cdot g}}{n^l_{CH_4} + x_{CH_4} \cdot \dfrac{p^{sat}_{CH_4} \cdot A}{M_{rCH_4} \cdot g} + n^l_{N_2} + \left(1 - x_{CH_4}\right)\dfrac{p^{sat}_{N_2} \cdot A}{M_{CH_4} \cdot g}} \tag{17}$$

where $n^l_{CH_4}$ and $n^l_{N_2}$ are the mole numbers of CH_4 and N_2 in the liquid phase, respectively. A is the surface area of Titan (Table 1).

Since the total mole number of N_2, $n^{tot}_{N_2}$, is given by

$$n^{tot}_{N_2} = n^{l}_{N_2} + n^{g}_{N_2} = \left(1 - x_{CH_4}\right)\left(n^{l}_{N_2} + n^{l}_{CH_4}\right) + \left(1 - x_{CH_4}\right)\frac{p^{sat}_{N_2} \cdot A}{M_{N_2} \cdot g} \tag{18}$$

the sum of mole numbers of CH_4 and N_2 in the liquid phase is

$$n^{l}_{N_2} + n^{l}_{CH_4} = \frac{n^{tot}_{N_2}}{1 - x_{CH_4}} - \frac{p^{sat}_{N_2} \cdot A}{M_{N_2} \cdot g}$$

With $x_{CH_4} = n^{l}_{CH_4}/(n^{l}_{CH_4} + n^{l}_{N_2})$ eq. 17 can now be rewritten as

$$\bar{x}_{CH_4} = \frac{x_{CH_4}\left[\dfrac{n^{tot}_{N_2}}{1 - x_{CH_4}} - \dfrac{p^{sat}_{N_2} \cdot A}{M_{N_2} \cdot g} + \dfrac{p^{sat}_{CH_4} \cdot A}{M_{CH_4} \cdot g}\right]}{x_{CH_4}\left[\dfrac{n^{tot}_{N_2}}{1 - x_{CH_4}} - \dfrac{p^{sat}_{N_2} \cdot A}{M_{N_2} \cdot g} + \dfrac{p^{sat}_{CH_4} \cdot A}{M_{CH_4} \cdot g}\right] + n^{tot}_{N_2}} \tag{19}$$

$\bar{x}_{CH_4}$ in eq. 19 depends on time through x_{CH_4}, the mole fraction of CH_4 in the liquid phase, all other parameters $p^{sat}_{CH_4}$, $p^{sat}_{N_2}$, M_{N_2}, M_{CH_4}, g and in particular $n^{tot}_{N_2}$ are constant, i.e., they do not depend on time provided the temperature is also independent of time.

Below the wavelength λ = 1650 Å, methane dissociates according to the reaction scheme presented in the introductory section with the destruction rate of $4 \cdot 10^{-12}$ kg m^{-2} = $2.5 \cdot 10^{-10}$ mol m^{-2} s^{-1} [1,2]. The total destruction rate on Titan is therefore $2.5 \cdot 10^{-10} \cdot 4\pi R_T^2 = 2.1 \cdot 10^4$ mol s^{-1}. The loss of CH_4 is proportional to the sunlight intensity I_S and the mole number of CH_4 in the atmosphere $n^{g}_{CH_4}$ (see eq. 16).

$$\begin{aligned} &\frac{dn^{t}_{CH_4}}{dt} = 2.1 \cdot 10^4 = -n^{g}_{CH_4} \cdot I_S \cdot k' = \\ &-k \cdot x_{CH_4}(t) \cdot p^{sat}_{CH_4} \cdot A / \left(M_{CH_4} \cdot g\right) \text{mol s}^{-1} \end{aligned} \tag{20}$$

with $I_S \cdot k' = k$ where $x_{CH_4}(t)$ is the mole fraction of CH_4 in the liquid phase at time t. From eq. 2, $x_{CH_4}(t = 0) = 0.698$ is the mole fraction of CH_4 in the liquid phase at present, and it follows

$$k = \frac{2.1 \cdot 10^4 \cdot M_{CH_4} \cdot g}{0.698 \cdot p^{sat}_{CH_4} \cdot A}$$

We now have to integrate eq. 20

$$\int_0^t \frac{dn^{tot}_{CH_4}}{x_{CH_4}(t)} = -K \cdot t \tag{21}$$

with

$$K = k \cdot \frac{p^{\mathrm{sat}}_{\mathrm{CH_4}} \cdot A}{M_{\mathrm{CH_4}} \cdot g} = 2.1 \cdot 10^4 / 0.698 = 3.0 \cdot 10^4 \,\mathrm{mol\ s^{-1}}$$

where the time t can be positive (future) or negative (past). Equation 21 with K = const implies that the luminosity of the sun has been constant all the time, which is a realistic assumption with exception of the early time of the solar system [2].

To solve the integral in eq. 21, we write

$$\mathrm{d}n^{\mathrm{tot}}_{\mathrm{CH_4}} = \left(\frac{\mathrm{d}n^{\mathrm{tot}}_{\mathrm{CH_4}}}{\mathrm{d}\bar{x}} \right) \cdot \left(\frac{\mathrm{d}\bar{x}}{\mathrm{d}x_{\mathrm{CH_4}}} \right) \mathrm{d}x_{\mathrm{CH_4}} \tag{22}$$

Considering that $n^{\mathrm{tot}}_{\mathrm{N_2}}$ = const, we obtain with $\bar{x} = n^{\mathrm{tot}}_{\mathrm{CH_4}}/(n^{\mathrm{tot}}_{\mathrm{CH_4}} + n^{\mathrm{tot}}_{\mathrm{N_2}})$

$$\frac{\mathrm{d}n^{\mathrm{tot}}_{\mathrm{CH_4}}}{\mathrm{d}\bar{x}} = \frac{\left(n^{\mathrm{tot}}_{\mathrm{CH_4}} + n^{\mathrm{tot}}_{\mathrm{N_2}} \right)^2}{n^{\mathrm{tot}}_{\mathrm{N_2}}} \tag{23}$$

and from differentiating eq. 19

$$\frac{\mathrm{d}\bar{x}_{\mathrm{CH_4}}}{\mathrm{d}x_{\mathrm{CH_4}}} = \frac{n^{\mathrm{tot}}_{\mathrm{N_2}} \left(\dfrac{n^{\mathrm{tot}}_{\mathrm{N_2}}}{\left(1 - x_{\mathrm{CH_4}}\right)^2} - \dfrac{p^{\mathrm{sat}}_{\mathrm{N_2}} \cdot A}{M_{\mathrm{N_2}} \cdot g} + \dfrac{p^{\mathrm{sat}}_{\mathrm{CH_4}} \cdot A}{M_{\mathrm{CH_4}} \cdot g} \right)}{\left[x_{\mathrm{CH_4}} \left(\dfrac{n^{\mathrm{tot}}_{\mathrm{N_2}}}{1 - x_{\mathrm{CH_4}}} - \dfrac{p^{\mathrm{sat}}_{\mathrm{N_2}} \cdot A}{M_{\mathrm{N_2}} \cdot g} + \dfrac{p^{\mathrm{sat}}_{\mathrm{CH_4}} \cdot A}{M_{\mathrm{CH_4}} \cdot g} \right) + n^{\mathrm{tot}}_{\mathrm{N_2}} \right]} \tag{24}$$

Since the denominator of eq. 24 is equal to $(n^{\mathrm{tot}}_{\mathrm{N_2}} + n^{\mathrm{tot}}_{\mathrm{CH_4}})^2$, substituting eq. 23 and eq. 24 into eq. 22 and then in eq. 21 gives

$$-Kt = \int_{x_{\mathrm{CH_4}}(t=0)}^{x_{\mathrm{CH_4}}(t)} \left(\frac{n^{\mathrm{tot}}_{\mathrm{N_2}}}{\left(1 - x_{\mathrm{CH_4}}\right)^2} - \frac{p^{\mathrm{sat}}_{\mathrm{N_2}} \cdot A}{M_{\mathrm{N_2}} \cdot g} + \frac{p^{\mathrm{sat}}_{\mathrm{CH_4}} \cdot A}{M_{\mathrm{CH_4}} \cdot g} \right) \cdot \frac{\mathrm{d}x_{\mathrm{CH_4}}}{x_{\mathrm{CH_4}}} \tag{25}$$

The integral in eq. 25 can be solved analytically, and the result is

$$-Kt = n^{\mathrm{tot}}_{\mathrm{N_2}} \left[\frac{1}{1 - x_{\mathrm{CH_4}}(t)} - \frac{1}{1 - x_{\mathrm{CH_4}}(t=0)} - \ln \left(\frac{1 - x_{\mathrm{CH_4}}(t)}{1 - x_{\mathrm{CH_4}}(t=0)} \right) \cdot \frac{x_{\mathrm{CH_4}}(t=0)}{x_{\mathrm{CH_4}}(t)} \right] + \frac{A}{g} \left(\frac{p^{\mathrm{sat}}_{\mathrm{CH_4}}}{M_{\mathrm{CH_4}}} - \frac{p^{\mathrm{sat}}_{\mathrm{N_2}}}{M_{\mathrm{N_2}}} \right) \cdot \ln \left(\frac{x_{\mathrm{CH_4}}(t)}{x_{\mathrm{CH_4}}(t=0)} \right) \tag{26}$$

Equations 19 and 26 are the basis for discussing the scenario.

The pressure of the $CH_4 + N_2$ mixture is given by

$$p\left(x_{\mathrm{CH_4}}\right) = x_{\mathrm{CH_4}}\left(p^{\mathrm{sat}}_{\mathrm{CH_4}} - p^{\mathrm{sat}}_{\mathrm{N_2}}\right) + p^{\mathrm{sat}}_{\mathrm{N_2}} \tag{27}$$

or

$$p\left(y_{\mathrm{CH_4}}\right) = \frac{y_{\mathrm{CH_4}} \cdot p^{\mathrm{sat}}_{\mathrm{N_2}}}{p^{\mathrm{sat}}_{\mathrm{CH_4}} + y_{\mathrm{CH_4}}\left(p^{\mathrm{sat}}_{\mathrm{N_2}} - p^{\mathrm{sat}}_{\mathrm{CH_4}}\right)} \cdot \left(p^{\mathrm{sat}}_{\mathrm{CH_4}} - p^{\mathrm{sat}}_{\mathrm{N_2}}\right) + p^{\mathrm{sat}}_{\mathrm{N_2}} \tag{28}$$

where $p(x_{\mathrm{CH_4}}) = p(y_{\mathrm{CH_4}})$ is the total pressure as function of $x_{\mathrm{CH_4}}$ or $y_{\mathrm{CH_4}}$, respectively.

In Fig. 4, $p(x_{\mathrm{CH_4}})$, $p(y_{\mathrm{CH_4}})$, and $p(\bar{x}_{\mathrm{CH_4}})$ with $\bar{x}_{\mathrm{CH_4}}$ taken from eq. 19 are plotted in a common diagram at 93 K. Three different values of $n^{\mathrm{tot}}_{\mathrm{N_2}}$ have been chosen for calculating $p(\bar{x}_{\mathrm{CH_4}})$: $n^{\mathrm{tot}}_{\mathrm{N_2}} = 3.08 \cdot 10^{20}$ mol corresponds to a surface of Titan which is covered by 4 % of lakes with a depth of 100 m, $n^{\mathrm{tot}}_{\mathrm{N_2}} = 3.39 \cdot 10^{20}$ mol has the same coverage but a depth of 1000 m. $n^{\mathrm{tot}}_{\mathrm{N_2}} = 10.16 \cdot 10^{20}$ mol corresponds to a coverage of 28 % and a depth of 600 m. This is exactly the value where $n^{g}_{\mathrm{N_2}} = n^{\mathrm{tot}}_{\mathrm{N}}$ when $x_{\mathrm{CH_4}}$ becomes zero according to eq. 16.

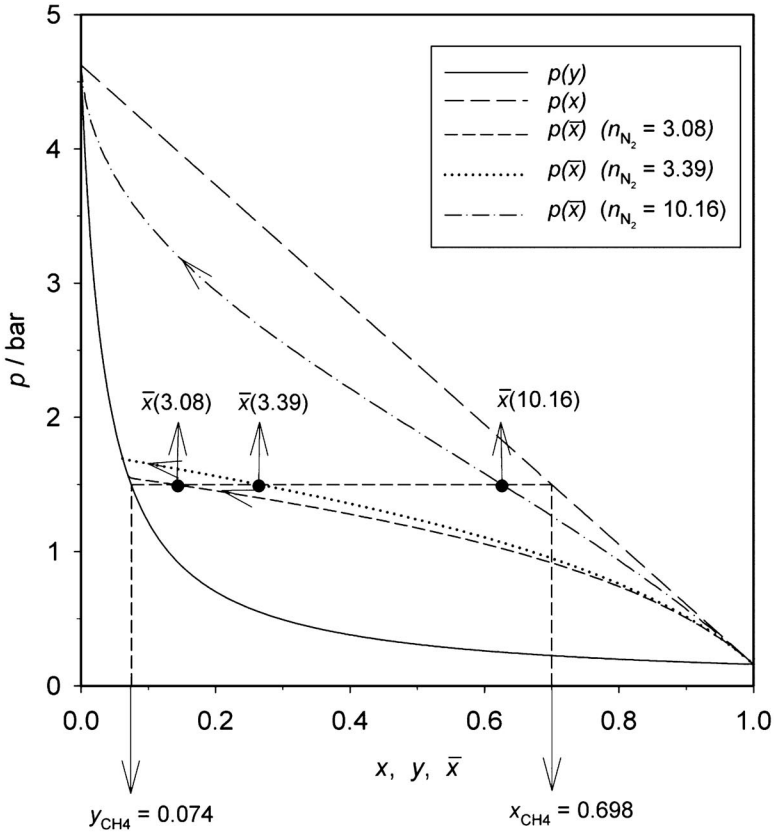

Fig. 4 Equilibrium *x*,*p* diagram of an ideal binary $CH_4 + N_2$ mixture with trajectories of the total mole fraction of CH_4 $\bar{x}$ at different total mole numbers of N_2 $n^{\mathrm{tot}}_{\mathrm{N_2}}$.

Figure 4 illustrates the "lever rule" of binary phase diagrams. For the present situation with $y_{CH_4} = 0.074$ and $x_{CH_4} = 0.698$ the dashed horizontal line indicates the 2-phase region with $\bar{x}_{CH_4}$-values corresponding to their $n^{tot}_{N_2}$-values. The higher $n^{tot}_{N_2}$ is the closer is $\bar{x}_{CH_4}$ to the value of x_{CH_4}. The $\bar{x}_{CH_4}$-trajectories indicated by arrows show how $\bar{x}_{CH_4}$ is changed with decreasing values of x_{CH_4}, i.e., with increasing time. It is interesting to note that the trajectories with $n^{tot}_{N_2} = 3.08 \cdot 10^{20}$ mol and $n^{tot}_{N_2} = 3.39 \cdot 10^{20}$ mol end on the $p(y_{CH_4})$-curve. This means that after a certain time, $\bar{x}_{CH_4}$ becomes equal to y_{CH_4}, and all liquid reservoirs on Titan would have disappeared. The surface has dried out and methane being now exclusively present in the atmosphere will be photochemically destructed according to a first-order kinetics. Finally, a dry atmosphere containing pure N_2 will survive. In the case of $n^{tot}_{N_2} = 10.16 \cdot 10^{20}$ mol the trajectory ends at $y_{CH_4} = \bar{x}_{CH_4} = x_{CH_4} = 0$ and at $p = p^{sat}_{N_2}$ which means that the atmosphere consists of pure N_2. For $n^{tot}_{N_2} > 10.16 \cdot 10^{20}$ mol the final situation will be an atmosphere of pure N_2 with $p = p^{N_2}_{sat}$ and liquid reservoirs with pure N_2 on the surface.

The explicit time evolution of x_{CH_4} obtained by eq. 26 is shown in Figs. 5 and 6. According to these results, $x_{CH_4} > 0.9$ can be expected at the time of Titan's formation ($4 \cdot 10^9$ years ago) for all values of $n^{tot}_{N_2}$ considered here.

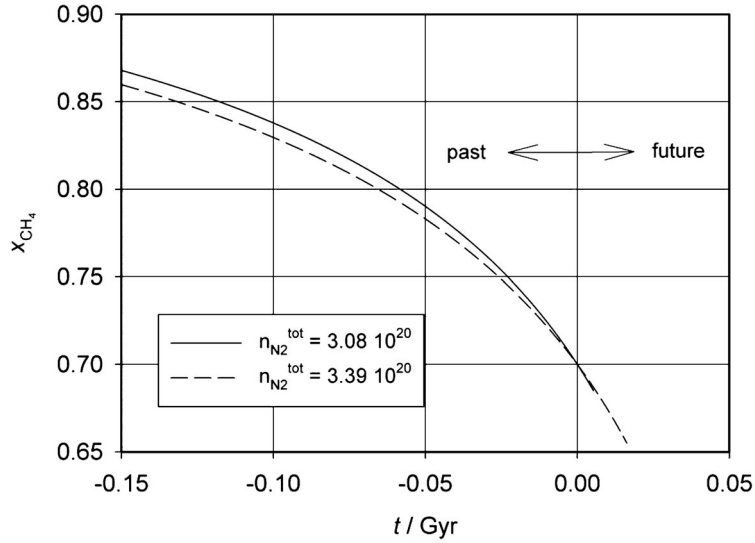

Fig. 5 Mole fraction $\bar{x}_{CH_4}$ in the liquid phase as function of time at fixed total mole numbers of N_2 on Titan's surface $n^{tot}_{N_2} = 3.08 \cdot 10^{20}$ mol and $n^{tot}_{N_2} = 3.39 \cdot 10^{20}$ mol.

According to Fig. 5, the lakes will have disappeared in 10^7 years ($n^{tot}_{N_2} = 3.08 \cdot 10^{20}$ mol) or in $2.3 \cdot 10^7$ years ($n^{tot}_{N_2} = 3.39 \cdot 10^{20}$ mol) with the "last drop" of a liquid composition $x_{CH_4} \approx 0.685$ or 0.655, respectively. At higher values of $n^{tot}_{N_2}$ the liquid mixtures phase would exist much longer since $n^{tot}_{CH_4}$ is also larger at the same composition. In the case of $n^{tot}_{N_2} = 10.16 \cdot 10^{20}$ mol and $n^{tot}_{N_2} = 25 \cdot 10^{20}$ mol (see Fig. 6) CH_4 would have disappeared at Titan in ca. $3.5 \cdot 10^8$ and $2 \cdot 10^9$ years, respectively, resulting in a pure N_2 atmosphere with liquid N_2 reservoirs ($n^{tot}_{N_2} = 10.16 \cdot 10^{20}$ mol).

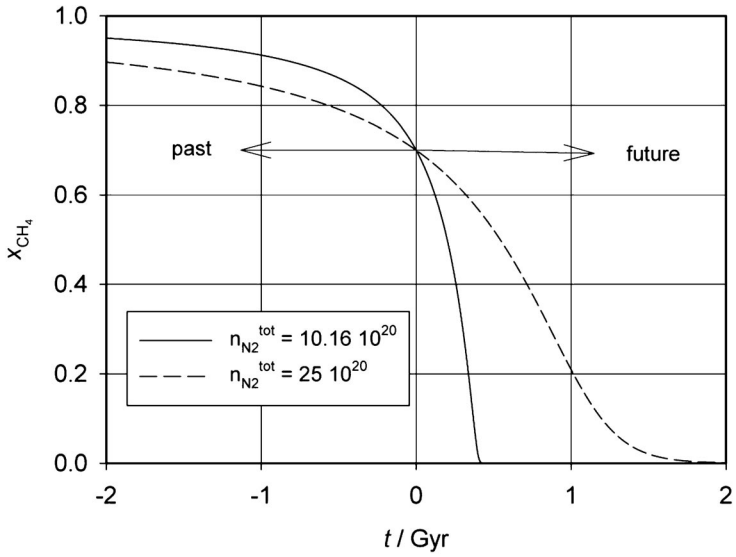

Fig. 6 Mole fraction x_{CH_4} in the liquid phase as function of time at fixed total mole numbers of N_2 on Titan's surface: $n_{N_2}^{tot} = 10.16 \cdot 10^{20}$ mol and $n_{N_2}^{tot} = 25 \cdot 10^{20}$ mol.

Figure 7 shows the change of the total amount of CH_4 $n_{CH_4}^{tot} = n_{CH_4}^{g} + n_{CH_4}^{l}$ on Titan as a function of time for the past and the future also based on the present values of $x_{CH_4} = 0.658$ and $y_{CH_4} = 0.074$ for different values of $n_{N_2}^{tot}$ as indicated. $n_{CH_4}^{tot}$ has been calculated by

$$n_{CH_4}^{tot}(t) = \frac{\bar{x}_{CH_4}(t)}{1 - \bar{x}_{CH_4}(t)} \cdot n_{N_2}^{tot}$$

with $\bar{x}_{CH_4} = \bar{x}_{CH_4}(x_{CH_4}(t))$ using eq. 19 with $x_{CH_4}(t)$ from eq. 26. According to the model, much more methane must have existed on Titan in the past than today, i.e., Titan has possibly been covered by a deep liquid ocean consisting of a $CH_4 + N_2$ mixture with distinctly higher concentrations of methane than today. It might also be possible that the amount of CH_4 and N_2 is already much higher at present than the detectable lakes on Titan's surface suggest due to hidden reservoirs such as "humidity" in micropores of Titan's icy crust.

The calculations of this simple scenario show that the fate of Titan's atmosphere and lakes sensitively depends on the amount and on the composition of liquid present today on Titan's surface. As long as there are no certain values available, neither the future nor the past can be predicted with acceptable reliability. If this situation is changed, the model of the scenario can be extended to real ternary mixture also including ethane. At this point, the purpose of this section was to demonstrate how scenario calculations can be performed.

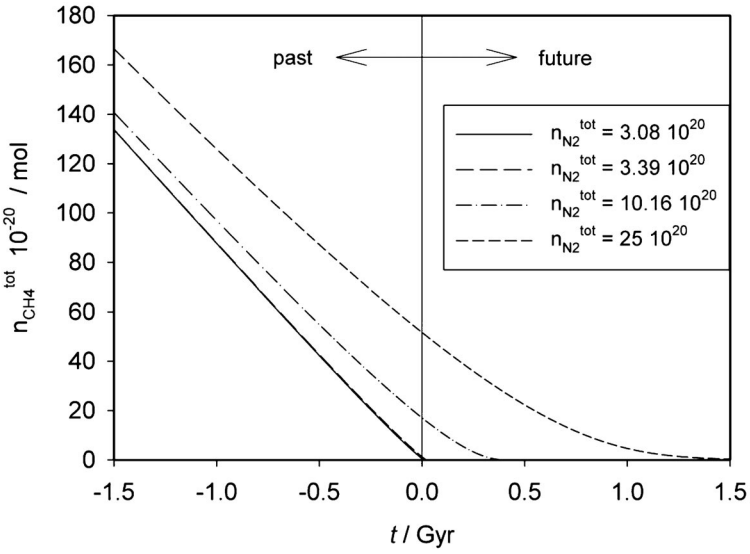

Fig. 7 Total mole number of CH_4 on Titan's surface as function of time at fixed total model numbers of N_2 as indicated.

TITAN'S INTERNAL STRUCTURE

As already mentioned, the low density indicates that Titan's interior must contain considerable amounts of water besides rocky material. Assuming that these different chemical components are well separated, we expect that Titan has an inner core consisting of rock, i.e., silicates, with an averaged density ρ_{rock} = 3 g m^{-3}, the mantel and the crust will mainly consist of liquid water and ice with an averaged density ρ_{N_2O} = 1.1 g m^{-3}. Accepting these figures, we are able to determine roughly the amount of water in the outer shell as well as the amount of silicate in the core. We also can calculate the central pressure and the pressure as function of radius r with $r = 0$ at the center. First, the radius r_1 of transition from the rocky material to the water phase is determined from the following mass balance:

$$m_{H_2O} + m_{rock} = \frac{4}{3}\pi <\rho> \cdot R_T^3 = \frac{4}{3}\pi\rho_{H_2O}\left[R_T^3 - r_1^3\right] + \frac{4}{3}\pi\rho_{rock} \cdot r_1^3 \tag{29}$$

where R_T is Titan's radius (see Table 1).

Solving eq. 29 for r_1^3 gives

$$r_1^3 = R_T^3 \frac{<\rho> - \rho_{H_2O}}{\rho_{rock} - \rho_{H_2O}} \tag{30}$$

Using the known data of $<\rho>$ = 1.88 g m^{-3} (see Table 1), ρ_{H_2O}, ρ_{rock}, and R_T the result is r_1 = 1913 km or r_1/R_T = 0.743.

This is a rough estimate because ρ_{H_2O} and ρ_{rock} are averaged values over the pressure and temperature profile of Titan's interior. Improved results can be obtained by considering values of compressibility and thermal expansion coefficients if these profiles would be known.

The mass fraction w_{H_2O} of H_2O in Titan is

$$w_{H_2O} = \rho_{H_2O}\left(R_T^3 - r_1^3\right) / \left[\rho_{H_2O}\left(R_T^3 - r_1^3\right) + \rho_{rock} \cdot r_1^3\right] = 0.345$$

and the corresponding mass fraction of rock is $w_{rock} = 1 - w_{H_2O} = 0.655$.

Using the hydrostatic equilibrium condition

$$dp = -\rho \cdot g \cdot dr \tag{31}$$

the pressure profile of Titan's interior can easily be calculated. Using the local gravity acceleration $g(r)$

$$g(r) = G \cdot \frac{m(r)}{r^2} = \frac{4}{3}\pi G \cdot \rho(r)$$

eq. 31 can be written as

$$dp = -G\rho^2(r) \cdot \frac{4}{3}\pi r \cdot dr \tag{32}$$

with the gravitational constant $G = 6.673 \cdot 10^{-11}$ [J m kg^{-2}] and ρ either ρ_{H_2O} or ρ_{rock}. Integration of eq. 32 gives the central pressure p_0 assuming that ρ_{H_2O} and ρ_{rock} are independent of the pressure p with $p(r = R_T) \approx 0$:

$$p_0 \frac{2}{3}\pi G\left[\rho_{N_2O}^2\left(1-(0.743)^2\right)+\rho_{rock} \cdot (0.743)^2\right] \cdot R_T^2 = 5.106 \cdot 10^9 \text{ Pa} = 51 \text{ kbar} \tag{33}$$

where $r_1/R_T = 0.743$ has been used.

The pressure p_1 at r_1 is

$$p_1 = p_0 - \rho_{rock}^2 \cdot \frac{2}{3} G \cdot r_1^2 = 0.502 \cdot 10^9 \text{ Pa} \cong 5 \text{ kbar} \tag{34}$$

The dependence of the pressure p on r is given by

$$p(r) = p_0 - \rho_{rock}^2 \cdot \frac{2}{3}\pi G \cdot r^2 \quad \left(\text{for } r \le 0.743\ R_T\right)$$

$$p(r) = p_0 + \left[\left(\rho_{H_2O}^2 - \rho_{rock}^2\right) \cdot \left(0.743 \cdot R_T\right)^2 - \rho_{H_2O}^2 \cdot r^2\right] \cdot \frac{2}{3}\pi G \quad \left(\text{for } r \ge 0.743\ R_T\right) \tag{35}$$

The upper layer of the aqueous system is the crust consisting of water ice up to a depth of ca. 200 km followed by a layer of liquid water up to the depth where the solid phase of rocky materials begins. The existence of solid and liquid water layers can be understood by inspecting the phase diagram of water shown in Fig. 8.

Figure 8 shows that the tentative $T(p)$ curve most probably intersects the solid–liquid equilibrium line of water at ca. 0.5 kbar and $r = 2300$ km. In the literature [27] there are also aqueous NH_3 solutions discussed instead of pure water, leading to a second solid phase of pure water which is likely to exist between $r = 2100$ km and $r = 1913$ km. The dependence of pressure p on calculated according to eq. 35 is shown in Fig. 9.

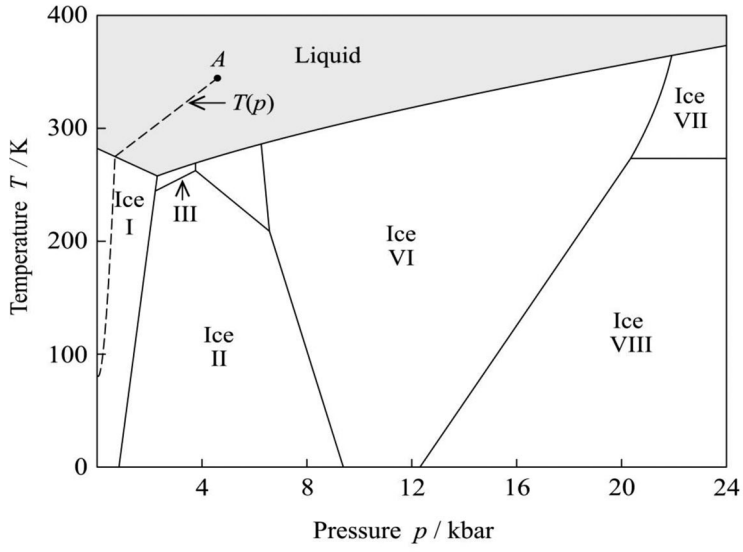

Fig. 8 Phase diagram of water. – – – – estimated $T(p)$ curve inside Titan. A = assumed transition point from aqueous phase to the rocky material.

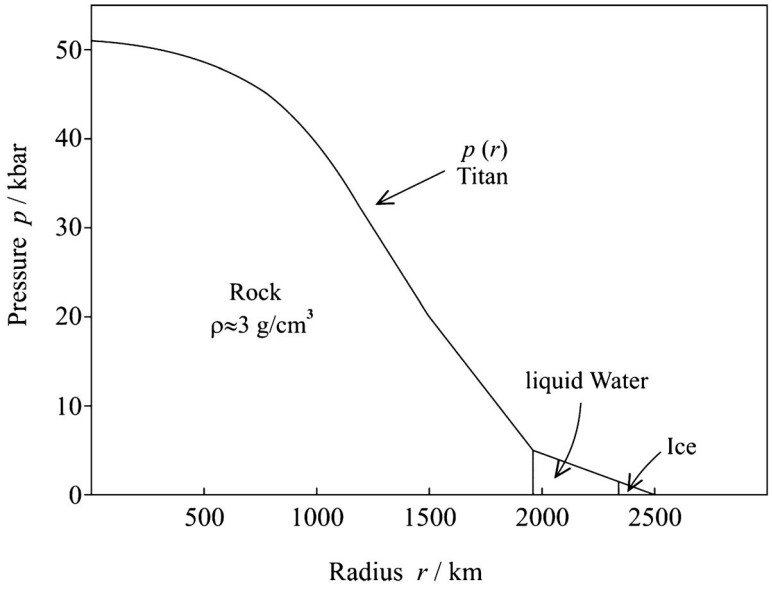

Fig. 9 Pressure as function of the distance from Titan's center.

CONCLUSIONS

- Using thermodynamic methods and comparatively simple theoretical tools, the composition of liquid lakes on Titan's surface can be predicted to be in acceptable agreement with the known atmospheric composition.
- The cloud ceiling of $CH_4 + N_2$ mixtures in the troposphere can be estimated. Depending on the degree of saturation on the bottom altitudes between 8 and 12 km are predicted provided the vapor

is not supersaturated. In the model calculations presented here a real mixture without ethane has been treated.

- A rough estimation of atmospheric scenarios in the past and the future can be made. The results depend essentially on the total amount of liquid on Titan's surface present today.
- An imagination of the internal structure of Titan can be provided predicting an aqueous mantle of ca. 700 km thickness and a hard core consisting of rocky material with a central pressure of ca. 51 kbar.

REFERENCES

1. J. S. Lewis. *Physics and Chemistry of the Solar System*, Academic Press, New York (1997).
2. Y. L. Yung, W. B. DeMore. *Photochemistry of Planetary Atmospheres*, Oxford University Press, Oxford (1999).
3. Y. L. Yung, M. Allen, J. P. Pinto. *Astrophys. J. Suppl. Ser.* **55**, 465 (1984).
4. R. D. Lorenz, Ch. P. McKay, J. I. Lunine. *Science* **275**, 642 (1997).
5. S. Atreya, E. Y. Adams, H. B. Niemann, J. E. Demick-Montelara, T. C. Owen, M. Fulchignoni, F. Ferri, E. H. Wilson. *Plant. Space Sci.* **54**, 1177 (2006).
6. E. R. Stofan, C. Elachi, J. I. Lunine, R. D. Lorenz, B. Stiles, K. L. Mitchell, S. Ostro, L. Sonderblom, C. Wood, Z. Zebker, S. Wall, M. Janssen, R. Kirk, R. Lopes, F. Paganelli, J. Radebaugh, L. Wye, Y. Anderson, M. Allison, R. Boehmer, P. Callahan, P. Encrenaz, E. Flamini, G. Francescetti, Y. Gim, G. Hamilton, S. Hensley, W. T. K. Johnson, K. Kellheher, D. Muhleman, P. Paillou, G. Picardi, F. Posa, L. Roth, R. Sen, S. Shaffer, S. Ventrella, R. West. *Nature* **445**, 61 (2007).
7. G. Mitri, A. P. Showman, J. I. Lunine, R. D. Lorenz. *Icarus* **186**, 385 (2007).
8. R. D. Lorenz, K. L. Mitchell, R. L. Kirk, A. G. Hayes, O. Aharonson, H. A. Zebker, P. Paillou, J. Radebaugh, J. I. Lunine, M. A. Janssen, S. D. Wall, R. M. Lopes, B. Stiles, S. Ostro, G. Mitri, E. R. Stofan. *Geophys. Res. Lett.* tbf35, L02206 (2008).
9. E. L. Barth, O. B. Toon. *Icarus* **162**, 93 (2003).
10. P. Rannou, F. Montmessin, F. Hourdin, S. Lebonnois. *Science* **311**, 201 (2006).
11. C. A. Griffith, P. Penteado, P. Rannou, R. Brown, V. Boudon, K. H. Baines, R. Clark, P. Drossart, B. Buratti, P. Nicholson, C. P. McKay, A. Coustenis, A. Negrao, R. Jaumann. *Science* **313**, 1620 (2006).
12. O. Mousis, B. Schmitt. *Astrophys. J.* **677**, 267 (2008).
13. H. B. Niemann, S. K. Arteya, S. J. Bauer, G. R. Carignan, J. E. Demick, R. L. Frost, D. Gautier, J. A. Haberman, D. N. Harpold, D. M. Hunten, G. Israel, J. I. Lunine, W. T. Kasprzak, T. C. Owen, M. Paulkovich, F. Raulin, E. Raaen, S. H. Way. *Nature* **438**, 779 (2005).
14. M. Fulchignoni, F. Ferri, F. Angrilli, A. J. Ball, A. Bar-Nun, M. A. Barucci, C. Bettanini, G. Bianchini, W. Borucki, G. Colombatti, M. Coradini, A. Coustenis, S. Debei, P. Falkner, G. Fanti, E. Flamini, V. Gaborit, R. Grard, M. Hamelin, A. M. Harri, B. Hathi, I. Jernej, M. R. Leese, A. Lehto, P. F. Lion Stoppato, J. J. López-Moreno, T. Mäkinen, J. A. M. McDonnell, C. P. McKay, G. Molina-Cuberos, F. M. Neubauer, V. Pirronello, R. Rodrigo, B. Saggin, K. Schwingenschuh, A. Seiff, F. Simoes, H. Svedhem, T. Tokano, M. C. Towner, R. Trautner, P. Withers, J. C. Zarnecki. *Nature* **438**, 785 (2005).
15. F. M. Flasar, R. K. Achterberg, B. J. Conrath, P. J. Gierasch, V. G. Kunde, C. A. Nixon, G. L. Bjoraker, D. E. Jennings, P. N. Romani, A. A. Simon-Miller, B. Bézard, A. Coustenis, P. G. J. Irwin, N. A. Teanby, J. Brasunas, J. C. Pearl, M. E. Segura, R. C. Carlson, A. Mamoutkine, P. J. Schinder, A. Barucci, R. Courtin, T. Fouchet, D. Gautier, E. Lellouch, A. Marten, R. Prangé, S. Vinatier, D. F. Strobel, S. B. Calcutt, P. L. Read, F. W. Taylor, N. Bowles, R. E. Samuelson, G. S. Orton, L. J. Spilker, T. C. Owen, J. R. Spencer, M. R. Showalter, C. Ferrari, M. M. Abbas, F. Raulin, S. Edgington, P. Ade, E. H. Wishnow. *Science* **308**, 975 (2005).

16. R. Prydz, R. D. Goodwin. *J. Chem. Thermodyn.* **4**, 127 (1972).
17. R. Span, E. W. Lemmon, R. T. Jacobsen, W. Wagner, A. Yokozeki. *J. Phys. Chem. Ref. Data* **29**, 1361 (2000).
18. D. Bücker, W. Wagner. *J. Phys. Ref. Data* **35**, 205 (2006).
19. R. C. Miller, A. J. Kidnay, M. J. Hiza. *AIChE J.* **19**, 145 (1973).
20. D. W. McClure, K. L. Lewis, R. C. Miller, L. A. K. Staveley. *J. Chem. Thermodyn.* **8**, 785 (1976).
21. M. Nunes da Ponte, W. B. Streett, L. A. K. Staveley. *J. Chem. Thermodyn.* **10**, 151 (1978).
22. Y.-P. Liu, R. C. Miller. *J. Chem. Thermodyn*. **4**, 85 (1972).
23. D. R. Massengill, R. C. Miller. *J. Chem. Thermodyn*. **5**, 207 (1973).
24. W. Wagner, K. M. deReuck (Eds.). *Methane-International Thermodynamic Tables of the Fluid State – 13*, Blackwell Science, Oxford (1996).
25. L. Kouvaris, F. M. Flasar. *Icarus* **91**, 112 (1991).
26. W. R. Thompson, J. A. Zollweg, D. H. Gabis. *Icarus* **97**, 187 (1992).
27. J. I. Lunine, D. J. Stevenson. *Icarus* **70**, 61 (1987).